PROCEEDINGS of the
23rd International Congress on Acoustics

9 to 13 September 2019 in Aachen, Germany

Integration of FEM shell elements as a “boundary condition” in BEM calculations using different solution methods

Ralf BURGSCHWEIGER[1]; Ingo SCHÄFER[2]; Martin OCHMANN[1]

[1] Beuth Hochschule für Technik Berlin, University of Applied Sciences, Faculty II, Research Group Computational Acoustics, 13353 Berlin,

[2] Bundeswehr Technical Center for Ships and Naval Weapons, Maritime Technology and Research (WTD71), Acoustic modelling (GF640), 24148 Kiel

ABSTRACT

Within the framework of research projects in the field of "Computational Acoustics", a powerful BEM-based code for the determination of the backscattered sound pressure level in the far field has been developed in recent years, using different solution methods (direct and iterative solver, fast multipole method, ray tracing method etc.).

This code has been extended so that in addition to the "classic" boundary conditions (pressure, normal velocity, impedance, inertial coupling, etc.), additional FEM shell conditions and thus elastic material properties can be taken into account. For this purpose, an additional FEM equation system is set up for the elements concerned which is integrated directly into the BEM equation system via appropriate transformation matrices.

The solution of this overall system can be done by means of direct equation solvers (based on a complete sparse matrix), by eigenvalue calculations or by the so-called Schur method (using iterative solvers).

The paper deals with the mathematical and physical fundamentals, shows the differences between the solution methods of the entire system and presents the results of test structures. As far as available until then, a comparison is also made with results from "pure" FEM calculations.

Keywords: FEM shell elements, BEM

1. INTRODUCTION

The calculation of the sound pressure in the far field for more complex structures of thin elastic shells, which are in liquid media and interact with them, is done for the low and middle frequency range mostly using the Finite Element Method (FEM). However, this is often no longer feasible with justifiable effort, especially for objects with larger dimensions.

Therefore, an already developed powerful BEM application has been extended to the possibility of defining thin shells as a "boundary condition" in the form of FEM shell elements, without the need for changes to the surface structures used.

This takes into account the elastic material properties of the thin shells and binds them directly into the BEM, without the need for additional applications or calculation steps.

2. BASICS AND FORMULATIONS

2.1 Used FEM shell elements and matrices

The presented method uses simple triangular planar FEM shell elements, which are assigned an elastic material and a shell thickness. The evaluation of the associated physical quantities (displacement W, rotation angles φ, forces F) takes place at the "corners" (nodes) of the elements.

For the calculation of the element-specific mass matrices $\mathbf{M}_v$ and stiffness matrices $\mathbf{K}_v$, the Kirchhoff method, as described in the formula work in [1], Chap. 7 and 8, is currently used.

These submatrices are inserted into the global sparse FEM matrices $\mathbf{M}_d$ and $\mathbf{K}_d$, ordered

[1] burgi@beuth-hochschule.de, ochmann@beuth-hochschule.de

[2] ingo5schaefer@bundeswehr.org

according to the above physical quantities, and combined within a frequency-dependent global FEM matrix $\mathbf{K}_f(\omega)$ of order $O(\mathbf{K}_f) = 6N_{no,fem} \times 6N_{no,fem}$ (Eq. (1)).

$$\mathbf{K}_f(\omega) = \mathbf{K}_d - \omega^2 \mathbf{M}_d = \begin{bmatrix} \overbrace{\mathbf{K}_{\varphi\varphi}}^{3N_{no,fem}} & \overbrace{\mathbf{K}_{\varphi w}}^{3N_{no,fem}} \\ \mathbf{K}_{w\varphi} & \mathbf{K}_{ww} \end{bmatrix} \tag{1}$$

This results in the frequency-dependent FEM equation system used for all solution variants:

$$\begin{bmatrix} \mathbf{K}_{\varphi\varphi} & \mathbf{K}_{\varphi w} \\ \mathbf{K}_{w\varphi} & \mathbf{K}_{ww} \end{bmatrix} \begin{bmatrix} \vec{\varphi} \\ \vec{W} \end{bmatrix} = \begin{bmatrix} 0 \\ -\vec{F} \end{bmatrix} \tag{2}$$

2.2 Used signs and symbols

$\mathbf{E}$	identity matrix
$\mathbf{S}_{el}$	Areas of the surface elements
$\mathbf{B}_{id}$	BEM matrix (indirect BEM, frequency-dependent, dense)
$\Delta\vec{p}_{id}$	Pressure difference (indirect BEM)
ρ	Density of the surrounding material
c	Sound velocity in the surrounding material
α_{BM}	Burton-Miller-factor
$\vec{v}_{inc}$	incident normal velocity
$N_{no,fem}$	Number of nodes at the FEM elements
$N_{el,id}$	Number of indirect BEM elements
$\mathbf{K}_f(\omega)$	FEM matrix (frequency dependent), also $\mathbf{K}_f$
$\vec{v}_{MVP,*}$	Matrix vector product part (depending on context)

2.3 Structure of the complete system of equations (in combination with the indirect BEM)

Within the BEM calculations, constant plane elements are used (collocation) and the physical quantities (Δp_{id}, v_n) are evaluated in the element center. The coupling with the node-based FEM components is made with two sparse transformation matrices ($\mathbf{T}_1$ and $\mathbf{T}_2$).

The method couples the FEM with the indirect BEM (identical fluid on both sides of the elements, as used within the inertial coupling method, see [2]) and leads to the following system of equations:

$$\begin{bmatrix} \mathbf{K}_{\varphi\varphi} & \mathbf{K}_{\varphi w} & 0 & 0 & 0 \\ \mathbf{K}_{w\varphi} & \mathbf{K}_{ww} & \mathbf{E} & 0 & 0 \\ 0 & 0 & \mathbf{E} & 0 & \mathbf{S}_{el}\mathbf{T}_2 \\ 0 & \mathbf{i}\omega\mathbf{T}_1 & 0 & \mathbf{E} & 0 \\ 0 & 0 & 0 & -\mathbf{E}\rho c & \mathbf{B}_{id} \end{bmatrix} \begin{bmatrix} \vec{\varphi} \\ \vec{W} \\ \vec{F} \\ \vec{v}_{id} \\ \Delta\vec{p}_{id} \end{bmatrix} = \begin{bmatrix} 0 \\ 0 \\ 0 \\ 0 \\ \alpha_{BM}\vec{v}_{inc} \end{bmatrix} \tag{3}$$

This can be simplified by eliminating $\vec{F}$ to

$$\begin{bmatrix} \mathbf{K}_{\varphi\varphi} & \mathbf{K}_{\varphi w} & 0 & 0 \\ \mathbf{K}_{w\varphi} & \mathbf{K}_{ww} & 0 & -\mathbf{S}_{el}\mathbf{T}_2 \\ 0 & \mathbf{i}\omega\mathbf{T}_1 & \mathbf{E} & 0 \\ 0 & 0 & -\mathbf{E}\rho c & \mathbf{B}_{id} \end{bmatrix} \begin{bmatrix} \vec{\varphi} \\ \vec{W} \\ \vec{v}_{id} \\ \Delta\vec{p}_{id} \end{bmatrix} = \begin{bmatrix} 0 \\ 0 \\ 0 \\ \alpha_{BM}\vec{v}_{inc} \end{bmatrix} \tag{4}$$

and by eliminating $\vec{v}_{id}$ to

$$\begin{bmatrix} \overbrace{\mathbf{K}_{\varphi\varphi}}^{3\times N_{no,fem}} & \overbrace{\mathbf{K}_{\varphi w}}^{3\times N_{no,fem}} & \overbrace{0}^{N_{el,id}} \\ \mathbf{K}_{w\varphi} & \mathbf{K}_{ww} & -\mathbf{S}_{el}\mathbf{T}_2 \\ 0 & \mathbf{i}\omega\rho c\mathbf{T}_1 & \mathbf{B}_{id} \end{bmatrix} \begin{bmatrix} \vec{\varphi} \\ \vec{W} \\ \Delta\vec{p}_{id} \end{bmatrix} = \begin{bmatrix} 0 \\ 0 \\ \alpha_{BM}\vec{v}_{inc} \end{bmatrix} \tag{5}$$

or in compressed form:

$$\begin{bmatrix} \mathbf{K}_f & -\mathbf{S}_{el}\mathbf{T}_2 \\ \mathbf{i}\omega\rho c\mathbf{T}_1 & \mathbf{B}_{id} \end{bmatrix} \begin{bmatrix} \vec{u} \\ \Delta\vec{p}_{id} \end{bmatrix} = \begin{bmatrix} 0 \\ \alpha_{BM}\vec{v}_{inc} \end{bmatrix}. \tag{6}$$

3. USED SOLUTION METHODS

Three different solution methods were implemented to take into account the FEM-specific material properties:

3.1 Combined sparse matrix (FULL SPARSE mode)

In this mode the total matrix of FEM and BEM coefficients according to Eq. (5) is completely build and solved using a direct solver for sparse matrices (Intel DSS direct sparse solver or PARDISO sparse solver).

Advantages:

- For so-called monostatic calculations with many right-hand sides according to the incident sound source position, only a one-time factorization of the combined matrix is required, and the subsequent solution process for each right-hand side is very fast.

Disadvantages:

- The memory requirement for the coefficients in a sparse matrix is higher (i.g. twice the size) since the BEM fraction $\mathbf{B}_{id}$ is fully populated and an additional column index is required per coefficient entry.
- During the factorization phase, sparse solvers require about 4 to 5 times the memory requirement of the output matrix. Since the solvers generally do not check this in advance, they may crash at this point.

3.2 Using the Schur method (SCHUR mode)

The basis of the Schur method is the simplified FEM equation system $\mathbf{K}_f$ according to Eq. (6). From this, $\vec{u}$ can be extracted

$$\vec{u} = -\mathbf{K}_f^{-1}\mathbf{S}_{el}\mathbf{T_2}\Delta\vec{p}_{id} \tag{7}$$

and the system of equations in Eq. (6) can be converted into

$$\left[-\mathbf{i}\omega\rho c\mathbf{T_1}\mathbf{K}_\mathrm{f}^{-1}\mathbf{S}_\mathrm{el}\mathbf{T_2} + \mathbf{B}_\mathrm{id}\right]\Delta\vec{\mathrm{p}}_\mathrm{id} = \alpha_\mathrm{BM}\vec{\mathrm{v}}_\mathrm{inc}. \tag{8}$$

An FEM coefficient matrix $\mathbf{J}_{sch,FEM}$ with

$$\mathbf{J}_\mathrm{sch,FEM} = \left[-\mathbf{i}\omega\rho c\mathbf{T_1}\mathbf{K}_\mathrm{f}^{-1}\mathbf{S}_\mathrm{el}\mathbf{T_2}\right]. \tag{9}$$

is build, which is added to the BEM matrix $\mathbf{B}_{id}$, and only

$$[\mathbf{B}_{id} + \mathbf{J}_{sch,FEM}][\Delta\vec{p}_{id}] = \alpha_{BM}\vec{v}_{inc} \tag{10}$$

has to be solved with a direct equation solver.

However, the formation of the inverse $\mathbf{K}_f^{-1}$ is very time-consuming and hardly usable in practice.

Alternatively, if an iterative solver is used for which matrix vector products are required per iteration vector $\vec{x}_i$ according to

$$\vec{b}_i(\vec{x}_i) = \vec{v}_{MVP,BEM}(\vec{x}_i) + \vec{v}_{MVP,sch}(\vec{x}_{i,FEM}), \tag{11}$$

the FEM matrix vector product part $\vec{v}_{MVP,sch}$ can be calculated much more simply by means of

$$\vec{v}_{MVP,sch}\left(\vec{x}_{i,FEM}\right) = -\mathbf{i}\omega\rho c\mathbf{T}_1\mathbf{K}_f^{-1}\mathbf{S}_\mathrm{el}\mathbf{T_2}\vec{x}_{i,FEM}. \tag{12}$$

In order to avoid the formation of $\mathbf{K}_f^{-1}$ at this point, an auxiliary vector

$$\vec{v}_{T2x} = \mathbf{S}_{el}\mathbf{T_2}\vec{x}_{i,FEM} \tag{13}$$

is generated and from this a Schur solution vector $\vec{v}_{sch}$ is calculated by solving the sparse system of equations

$$\mathbf{K}_f\vec{v}_{sch} = \vec{v}_{T2x} \tag{14}$$

with the aid of a sparse solver. This simplifies Eq. (12) to

$$\vec{v}_{MVP,sch}\left(\vec{x}_{i,FEM}\right) = -i\omega\rho c\mathbf{T}_1\vec{v}_{sch}. \tag{15}$$

Since $\mathbf{K}_f$ from Eq. (14) has to be factorized only once and then only has to be solved per iteration vector $\vec{x}_i$, the computing time per iteration is much lower.

Advantages:

- Only the memory required for the BEM matrix $\mathbf{B}_{id}$ is needed, the additional $\mathbf{J}_{sch,FEM}$ values are added up. Also, the amount of memory required for factorization usually does not increase for an equation solver for dense matrices.
- When using iterative solvers, the required matrix vector product parts of Eq. (11) can be prepared by rapid approximate methods, such as the fast multipole method (MLFMM). This will make significantly larger numbers of elements possible.

Disadvantages:

- For frequency sweeps, $\mathbf{K}_f$ and $\vec{v}_{sch}$ from Eq. (14) must be reassembled in accordance with Eq. (1) and factorized for each frequency.

3.3 Using eigenvalues (EIGEN mode)

In this mode, a predefined number N_{ev} of eigenvalues or vectors based on the frequency-independent FEM matrices $\mathbf{M}_d$ and $\mathbf{K}_d$ from Eq. (1) is determined by a so-called eigenvalue solver and stored in an eigenvalue matrix $\mathbf{\Psi}_{ev}$.

Using these matrices, two "small" square frequency-independent diagonal matrices $\mathbf{K}_{ev}$ and $\mathbf{M}_{ev}$ are formed by means of

$$\mathbf{K}_{ev} = \mathbf{\Psi}_{ev}^T \cdot \mathbf{K}_d \cdot \mathbf{\Psi}_{ev} \text{ and} \tag{16}$$

$$\mathbf{M}_{ev} = \mathbf{\Psi}_{ev}^T \cdot \mathbf{M}_d \cdot \mathbf{\Psi}_{ev} \tag{17}$$

with the order of $\mathcal{O}(\mathbf{K}_{ev}) = \mathcal{O}(\mathbf{M}_{ev}) = N_{ev}$.

The eigenvalue matrix $\mathbf{\Psi}_{ev}$ is then reduced to its "lower" half (belonging to the displacement $\vec{W}$) ($\mathbf{\Psi}_{ev,w}$), since the rotation angles are now no longer needed, and two auxiliary matrices $\mathbf{Q}_1$ and $\mathbf{Q}_2$ are generated by

$$\mathbf{Q}_1 = \mathbf{T}_1 \cdot \mathbf{\Psi}_{ev,w} \text{ and} \tag{18}$$

$$\mathbf{Q}_2 = \mathbf{\Psi}_{ev,w}^T \cdot \mathbf{S}_{el} \cdot \mathbf{T}_2. \tag{19}$$

Now, a frequency-dependent matrix $\mathbf{D}_{ev}$ is generated by means of

$$\mathbf{D}_{ev} = (\mathbf{K}_{ev} - \omega^2 \mathbf{M}_{ev})^{-1}, \tag{20}$$

whereby the formation of the inverse here is not so time-consuming due to the "small" order of $\mathcal{O}(\mathbf{D}_{ev}) = N_{ev} \times N_{ev}$.

From this, an auxiliary matrix $\mathbf{Q}_{D2}$ is generated by means of

$$\mathbf{Q}_{D2} = \mathbf{i}\omega(\mathbf{D}_{ev} \cdot \mathbf{Q}_2). \tag{21}$$

The matrix-matrix product of these auxiliary matrices is given by

$$\mathbf{J}_{ev,FEM} = \rho c \mathbf{Q}_1 \mathbf{Q}_{D2}. \tag{22}$$

As in the Schur method, it corresponds to an FEM coefficient matrix of the same order as that of the BEM matrix and is added to it, so that finally only the system of equations

$$[\mathbf{B}_{id} + \mathbf{J}_{ev,FEM}][\Delta\vec{p}_{id}] = \alpha_{BM}\vec{v}_{inc} \tag{23}$$

must be solved.

Advantages:

- As with the Schur method, only the memory needed for the fully populated BEM matrix $\mathbf{B}_{id}$ is required.
- For frequency sweeps, the eigenvalues need to be determined only once (based on the highest desired frequency), accordingly, the time required decreases after the first for all following frequencies. Furthermore, only the frequency-independent auxiliary matrices $\mathbf{Q}_1$ and $\mathbf{Q}_2$ must be "saved", all other variables can be discarded to save memory space.
- Using an iterative solver (e.g., GMRES), the time-consuming formation of the $\mathbf{J}_{ev,FEM}$ c oefficients can be replaced by a FEM MVP part $\vec{v}_{MVP,eig}$:

$$\vec{b}_i(\vec{x}_i) = \vec{v}_{MVP,BEM}(\vec{x}_i) + \vec{v}_{MVP,eig}(\vec{x}_{i,FEM}) \tag{24}$$

This can be calculated very quickly by means of

$$\vec{v}_{MVP,eig}\left(\vec{x}_{i,FEM}\right) = \rho c \mathbf{Q}_1 \mathbf{Q}_{D2} \vec{x}_{i,FEM}, \tag{25}$$

since the order of the matrices $\mathbf{Q}_1$ and $\mathbf{Q}_{D2}$ is significantly smaller than that of $\mathbf{B}_{id}$, while the BEM component

$$\vec{v}_{MVP,BEM}(\vec{x}_i) = \mathbf{B}_{id}\vec{x}_i \tag{26}$$

is conventionally calculated.

- Here too, in the case of iterative solvers, the required matrix vector products of Eq. (26) can be formed by rapid approximate methods.
- It is possible to determine the eigenvalues for individual FEM areas separately, this can lead to a lower number of required eigenvalues and thus reduce the time required.

Disadvantages:

- The number of eigenvalues N_{ev} required for a good quality of the solution can be estimated poorly in advance, since this strongly depends on the model and the boundary conditions. Accordingly, this specification must be checked manually and, if necessary, be increased adaptively, in which case the time required to determine the eigenvalues also increases disproportionately.

4. RESULTS FOR A FREQUENCY SWEEP

4.1 Used model

The model used (Figure 1) consists of a conical shell made of 6,058 triangular elements with a radius of 1 m, a thickness of 1 cm and steel as material, surrounded by water.

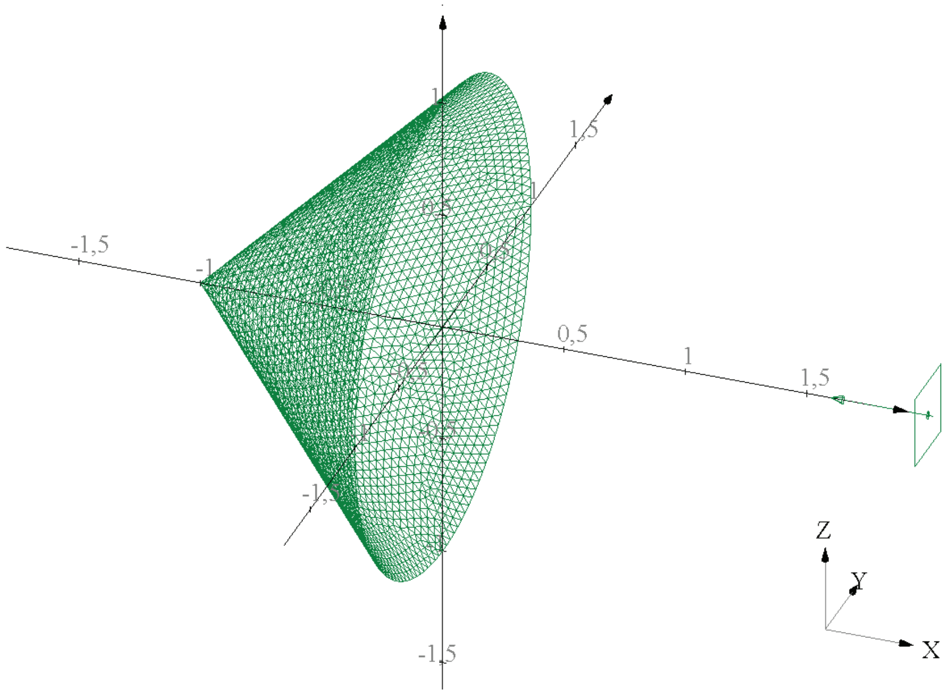

Figure 1 - used model

A plane incident wave in the negative X direction is used as a sound source to compare the results with the FEM COMSOL application, which gives a shorter calculation time due to the rotational symmetry.

4.2 Results

For a frequency range of 100 Hz to 1 kHz, the normalized sound pressure level in the far field was determined in 0.5 Hz increments (N_f = 1,801 frequencies) at a monostatic evaluation point at position [10, 0, 0 km] in order to be able to clearly recognize occurring resonances (Figure 2).

The maximum allowable relative error for the iterative solvers (b, d, g) has been set to 10^{-4}.

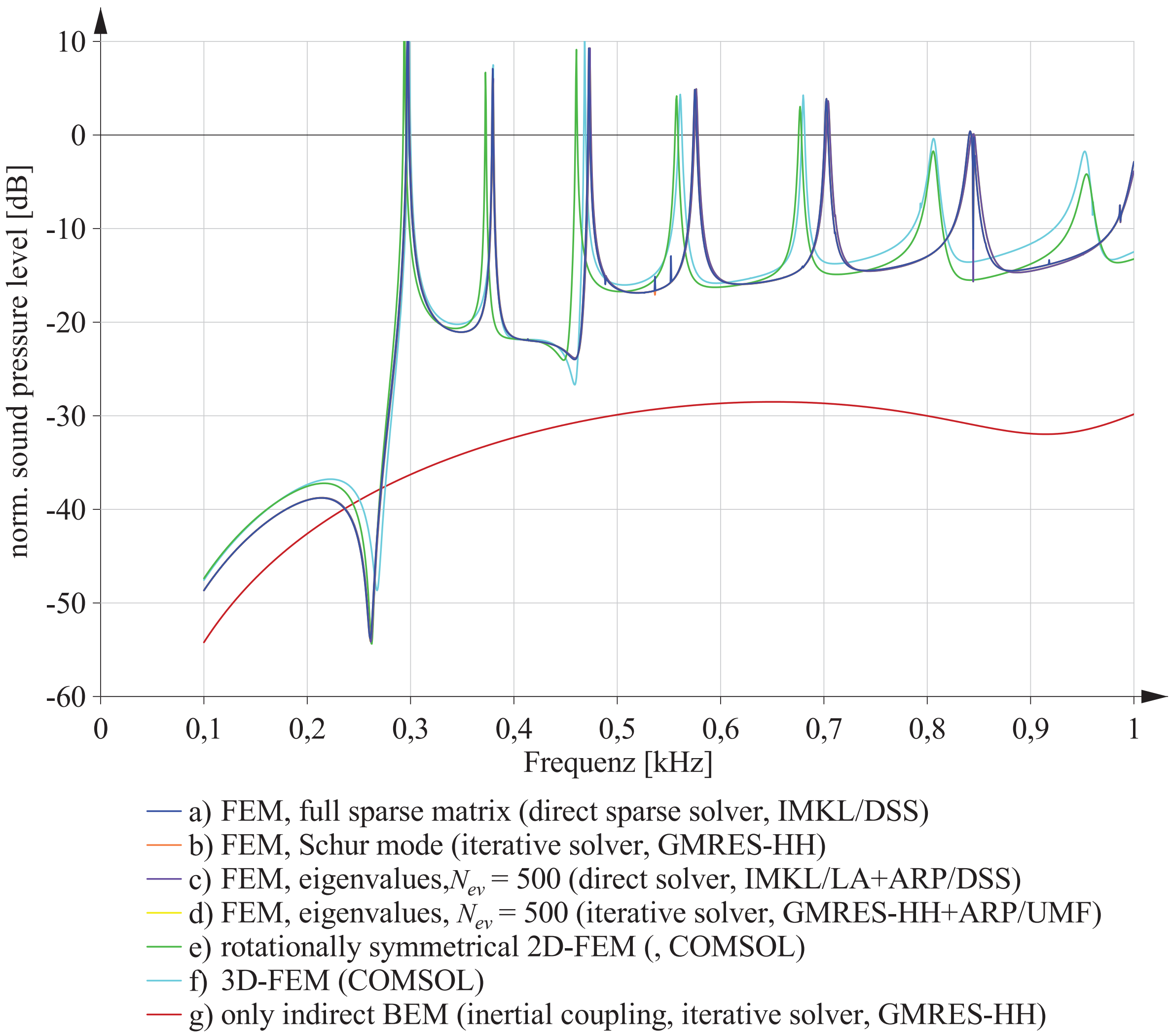

Figure 2 - Sound pressure level at a monostatic evaluation point at position [10, 0, 0] km (f = 100 … 1,000 Hz, Δf = 0,5 Hz, N_f = 1,801)

All three FEM calculation variants (full sparse matrix, eigenvalues and Schur method, a ... d) agree very well, the differences are, except for some isolated spikes at some frequencies, below one dB.

The difference to the indirect BEM (g) using the thin-shell inertial coupling method according to [2] is clearly seen and shows the great influence of the elastic material properties.

In comparison to the FEM results of COMSOL (e, f), a frequency shift appears with increasing frequency (with similar maxima and minima values). This is due to the different methods for calculating the FEM matrices (Kirchhoff method in our inhouse code, Reissner-Mindlin method in COMSOL) and requires further investigation. For better comparability, therefore, an additional implementation of the Reissner-Mindlin method for the own code is currently being prepared.

For information, Table 1 gives the calculation times for the different results.

The solution time of the FULL SPARSE variant is not significantly greater here than in the other methods due to the "small" number of elements.

Table 1 - Calculation times for the frequency sweep

Method / mode	**Calculation time** [h:m:s]
a) FULL SPARSE (direct)	3:48:55
b) SCHUR-Modus (iterative)	2:57:57
c) EIGEN-Modus (direct)	2:17:00
d) EIGEN-Modus (iterative)	1:37:16
e) 2D-FEM (COMSOL, rotationally symmetrical!)	0:07:12
f) 3D-FEM (COMSOL)	ca. 13 h
g) only indirect BEM (iterative)	0:21:52

4.3 Pressure differences at resonance points

To illustrate the changes in the difference of the pressure on both sides of the elements at the resonance points, the following figures show the real part of the pressure difference $\Re(\Delta p_{el,FEM})$ on the surface in the region around the first resonance point between 294 and 299 Hz.

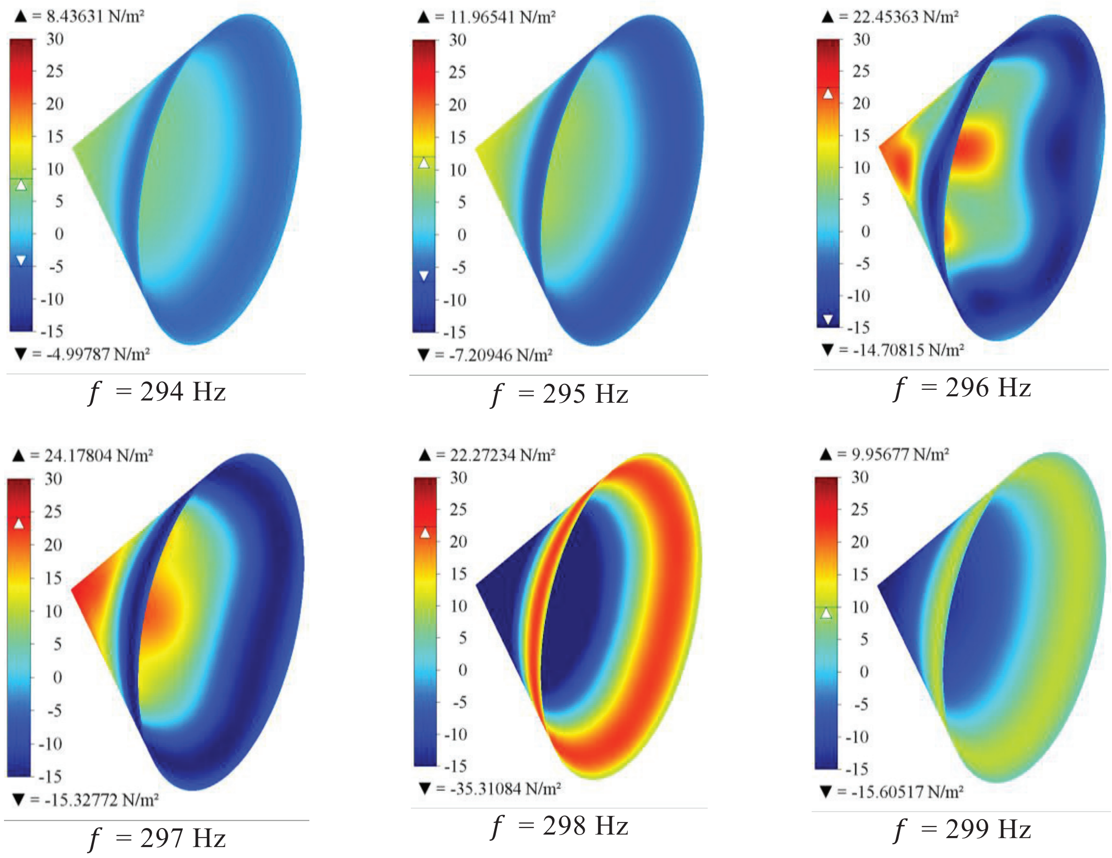

Figure 3 - $\Re(\Delta p_{el,FEM})$, real part of the pressure difference on the surface

The same value and color range (-15 ... +30 N/m²) is used in all 6 subfigures, so that it is easy to see how the pressure difference in the area around the resonance point increases significantly at approx. f = 297.15 Hz and then decreases again. Also the sign of the real part changes.

5. SUMMARY AND OUTLOOK

The implemented FEM coupling methods show good agreement with each other and in comparison with commercial FEM applications.

The speed advantage when using the BEM instead of the FEM in 3D is clearly visible.

The use of iterative equation solvers in conjunction with the implemented SCHUR or EIGEN solution variants enables the combination with the multi-level fast multipole method.

The code is currently being expanded for FEM shell boundary conditions with respect to closed structures, i.e., there is a vacuum inside the corresponding structural part.

Also in the future, the combination of arbitrary boundary conditions within the same model should be possible, as well as the "tight clamping" of existing edges.

REFERENCES

1. Steinke, P., Finite-Elemente-Methode; Rechnergestützte Einführung, 5. Auflage, Springer Vieweg Verlag, 2015, ISBN 978-3-642-53936-7.
2. Burgschweiger, R., Schäfer, I. and Ochmann, M., Implementation and results of a mass inertia coupling as an extension of the BEM for thin shells, Proceedings of the 22nd International Congress on Sound and Vibration (ICSV22), Florence, Italy (07/2015).
3. Burgschweiger, R., Schäfer, I. and Ochmann, M., Integration von FEM-Schalenelementen als Randbedingungen in BEM-Berechnungen unter Verwendung verschiedener Lösungsmethoden, Proceedings of the 45nd Deutsche Jahrestagung für Akustik (DAGA2019), Rostock, Germany (03/2019).